

REPORTS

crimination between the inner and outer trimannose structures by preventing binding to the inner branch point mannose. Selective binding of DC-SIGN and DC-SIGNR to the outer branched trimannose moiety can explain almost all of their binding characteristics (16).

Mannose-binding proteins (MBPs) are C-type lectins that function in innate immunity by recognizing carbohydrate structures characteristic of pathogens, and they do not bind strongly to mannose-type ligands present on host cell surfaces (5). Although the CRDs of DC-SIGN and DC-SIGNR share 24% sequence identity with rat serum MBP, the mode of binding of oligosaccharides to MBP is quite distinct from the interaction of DC-SIGN and DC-SIGNR with the branched trimannose structure. Each CRD in MBP interacts with a single terminal mannose or GlcNAc residue in an oligosaccharide ligand, and the rest of the oligosaccharide points away from the surface of the protein (17) (Fig. 2B). The architecture of the MBP trimer places the binding sites in the three CRDs far enough apart that MBP binds with high avidity only to the repetitive and dense arrays presented on pathogenic cell surfaces, but not to the more closely spaced terminal mannose residues present on endogenous oligosaccharides (18). In contrast, the interactions of DC-SIGN and DC-SIGNR with endogenous glycans on T cells and the HIV envelope result from high affinity binding to a characteristic internal feature of high-mannose oligosaccharides.

DC-SIGN- and DC-SIGNR-gp120 interactions represent a potential target for anti-HIV therapy aimed at disrupting the DC-virus interaction at primary sites of infection, in order to lower the efficiency of T cell infection. Although the high avidity generated by clustering low-affinity lectin monomers into oligomeric structures has made it difficult to design drugs aimed at disrupting protein-carbohydrate interactions, the unusually high affinity between the monomeric DC-SIGN or DC-SIGNR CRDs and high-mannose oligosaccharides (4) suggests that they may be useful targets. The mechanistic basis of the DC-SIGN- and DC-SIGNR-oligosaccharide interactions presented here provides a starting point for design of such therapeutics, which would attack the viral infection at a novel stage and which could potentially be prophylactic. Lastly, these studies suggest that the interaction of DC-SIGN and DC-SIGNR with endogenous ligands may not be restricted to ICAMs that have been studied to date, but may include other cell surface or soluble glycoproteins with appropriately displayed high mannose oligosaccharides.

References and Notes

1. J. Banchereau, R. M. Steinman, *Nature* **392**, 245 (1998).
2. T. B. H. Geijtenbeek *et al.*, *Cell* **100**, 575 (2000).
3. T. B. H. Geijtenbeek *et al.*, *Nature Immunol.* **1**, 353 (2000).
4. D. A. Mitchell, A. J. Fadden, K. Drickamer, *J. Biol. Chem.* **276**, 28939 (2001).
5. W. I. Weis, M. E. Taylor, K. Drickamer, *Immunol. Rev.* **163**, 19 (1998).
6. E. J. Soilleux, R. Barten, J. Trowsdale, *J. Immunol.* **165**, 2937 (2000).
7. S. Pöhlmann *et al.*, *Proc. Natl. Acad. Sci. U.S.A.* **98**, 2163 (2001).
8. A. A. Bashirova *et al.*, *J. Exp. Med.* **193**, 671 (2001).
9. T. B. H. Geijtenbeek *et al.*, *Cell* **100**, 587 (2000).
10. S. Pöhlmann *et al.*, *J. Virol.* **75**, 4664 (2001).
11. Supplemental data are available on Science Online at www.sciencemag.org/cgi/content/full/294/5549/2163/DC1.
12. K. Drickamer, *Curr. Opin. Struct. Biol.* **9**, 585 (1999).
13. A. J. Petrescu, S. M. Petrescu, R. A. Dwek, M. R. Wormald, *Glycobiology* **9**, 343 (1999).
14. T. Mizuochi *et al.*, *J. Biol. Chem.* **265**, 8519 (1990).
15. R. J. Woods, A. Pathiaseril, M. R. Wormald, C. J. Edge, R. A. Dwek, *Eur. J. Biochem.* **258**, 372 (1998).
16. The weak interaction with a GlcNAc-terminated neoglycolipid derived from an asialo, aglacto-bantennary N-linked glycan can be explained by the interaction of a terminal GlcNAc residue with the principal Ca²⁺ site, as observed in the cross-linked pairs of CRDs of DC-SIGN (Fig. 3B). This interpretation is confirmed by the observation that the corresponding galactose-terminated structure, in which the 4-OH of GlcNAc is inaccessible, does not bind at all. Moreover, modeling of a further mannose residue in α 1-2 linkage to the Man α 1-3Man arm of the trimannosyl moiety suggests that it would pack against Val³⁵¹ of DC-SIGN, whereas no contact would be made with the smaller Ser³⁶³ present at this position of DC-SIGNR. This

- observation may be related to the larger affinity difference between Man α and smaller oligosaccharides displayed by DC-SIGN relative to DC-SIGNR [see (4) and table 2 of supplemental data (11)].
17. W. I. Weis, K. Drickamer, W. A. Hendrickson, *Nature* **360**, 127 (1992).
 18. W. I. Weis, K. Drickamer, *Structure* **2**, 1227 (1994).
 19. A. Nicholls, GRASP: Graphical Representation and Analysis of Surface Properties (Columbia University, New York, 1992).
 20. Z. Otwinowski, W. Minor, *Methods Enzymol.* **276**, 307 (1997).
 21. R. A. Laskowski, M. W. MacArthur, D. S. Moss, J. M. Thornton, *J. Appl. Crystallogr.* **26**, 283 (1993).
 22. We thank E. Soilleux for providing cDNAs; D. Torgersen for assistance with protein preparation; G. Golan, O. Livnah, and G. Shoham of the Hebrew University for assistance with data collection; and L. Tong for the COMO program. Some of this work is based upon research conducted at the Stanford Synchrotron Radiation Laboratory (SSRL), a national facility operated by Stanford University for the DOE, Office of Basic Energy Sciences. The SSRL Structural Molecular Biology Program is supported by the Department of Energy, Office of Biological and Environmental Research and by the National Center for Research Resources, Biomedical Technology Program and National Institute of General Medical Sciences, NIH. Part of this research was carried out at the National Synchrotron Light Source, Brookhaven National Laboratory, which is supported by the DOE, Division of Materials Sciences and Division of Chemical Sciences. Supported by grants 041845 and 054508 from the Wellcome Trust (K.D.), and grant GM50565 from the NIH (W.I.W.). Coordinates and structure factors have been deposited in the Protein Data Bank, with accession codes 1K9J (DC-SIGN) and 1K9J (DC-SIGNR).

19 September 2001; accepted 1 November 2001

A Transgenic Model of Visceral Obesity and the Metabolic Syndrome

Hiroaki Masuzaki,¹ Janice Paterson,^{2,3} Hiroshi Shinyama,¹ Nicholas M. Morton,² John J. Mullins,³ Jonathan R. Seckl,² Jeffrey S. Flier^{1*}

The adverse metabolic consequences of obesity are best predicted by the quantity of visceral fat. Excess glucocorticoids produce visceral obesity and diabetes, but circulating glucocorticoid levels are normal in typical obesity. Glucocorticoids can be produced locally from inactive 11-keto forms through the enzyme 11 β hydroxysteroid dehydrogenase type 1 (11 β HSD-1). We created transgenic mice overexpressing 11 β HSD-1 selectively in adipose tissue to an extent similar to that found in adipose tissue from obese humans. These mice had increased adipose levels of corticosterone and developed visceral obesity that was exaggerated by a high-fat diet. The mice also exhibited pronounced insulin-resistant diabetes, hyperlipidemia, and, surprisingly, hyperphagia despite hyperleptinemia. Increased adipocyte 11 β HSD-1 activity may be a common molecular etiology for visceral obesity and the metabolic syndrome.

Obesity is associated with adverse metabolic consequences such as diabetes and dyslipidemia (1). The best predictor of these morbidities is not the total body adipose mass, but the specific quantity of visceral fat (2, 3). A molecular basis for disproportionate accumulation of visceral fat has not been identified

and the extent to which visceral adiposity causes or merely reflects the associated metabolic syndrome, which includes insulin resistance, glucose intolerance, and dyslipidemia, remains unclear (3).

One identified cause of visceral obesity and metabolic complications is exposure to

REPORTS

excessive levels of glucocorticoids. Although systemic glucocorticoid excess in rare Cushing's syndrome causes visceral obesity and the metabolic syndrome (4, 5), circulating glucocorticoid levels are normal in patients with the prevalent forms of obesity (5). However, glucocorticoid action on

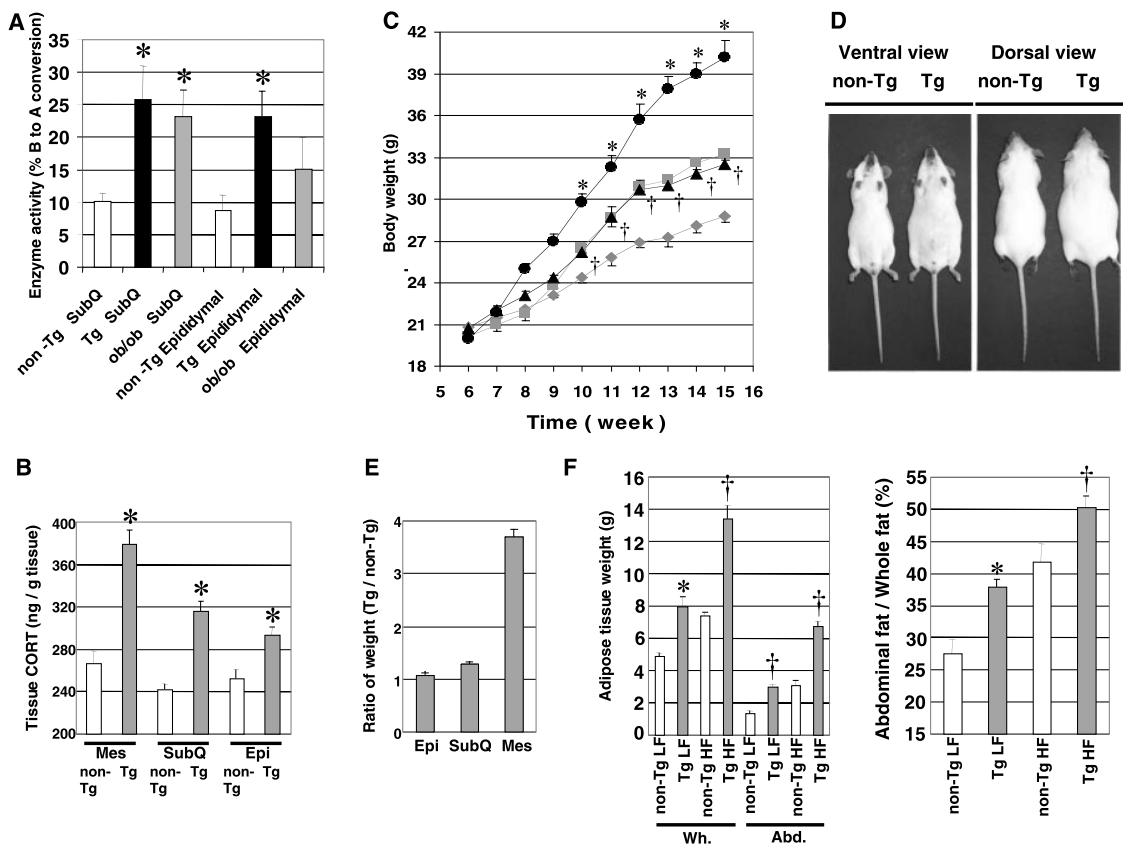
target tissues depends on both circulating hormone levels and intracellular prereceptor metabolism (6). The enzyme 11 β hydroxysteroid dehydrogenase type 1 (11 β HSD-1) plays a pivotal role in determining intracellular glucocorticoid concentrations by regenerating active glucocorticoid (cortisol in humans, corticosterone in rats and mice) from inactive cortisone and 11-dehydrocorticosterone (6-8) and has been suggested to serve as a tissue-specific amplifier of glucocorticoid action (6).

Mice homozygous for a targeted deletion of the 11 β HSD-1 gene are viable and developmentally normal but cannot regenerate active corticosterone from inert 11-dehydrocorticosterone in vivo, demonstrating that 11 β

HSD-1 is the sole 11 β -reductase in the body (9). The 11 β HSD-1-deficient mice show attenuated activation of glucocorticoid-sensitive hepatic gluconeogenic enzymes in response to stress or high-fat diets and have a diabetes-resistant phenotype (9). Recently, adipose tissue from obese humans has been shown to have increased 11 β HSD-1 activity (7). To test the hypothesis that increased production of glucocorticoid exclusively within adipose tissue would produce visceral obesity and features of the metabolic syndrome, we created transgenic mice overexpressing 11 β HSD-1 under the control of the enhancer-promoter region of the adipocyte fatty acid binding protein (aP2) gene (Web fig. 1) (10-12).

¹Division of Endocrinology and Metabolism, Department of Medicine, Beth Israel Deaconess Medical Center and Harvard Medical School, 330 Brookline Avenue, Boston, MA, 02215, USA. ²Endocrinology Unit, Molecular Medicine Center, University of Edinburgh, Edinburgh, EH4 2XU, Scotland, UK. ³Molecular Physiology Laboratory, University of Edinburgh, Edinburgh, EH8 9AG, Scotland, UK.
*To whom correspondence should be addressed. E-mail: jflie@caregroup.harvard.edu

Fig. 1. Creation of transgenic mice overexpressing 11 β HSD-1 in adipose tissue. The Institutional Animal Care and Use Committee (Beth Israel Deaconess Medical Center and Harvard Medical School, Boston, MA) approved all studies. (A) The 11 β HSD-1 activity in adipose tissue from transgenic mice (Tg) (male, 18 weeks of age, $n = 6$), non-transgenic littermates (non-Tg, $n = 6$), and age-matched male *ob/ob* mice ($n = 3$). Values were expressed as mean \pm SEM. SubQ, subcutaneous abdominal fat. In adipose tissue homogenates, the reaction catalyzed by 11 β HSD-1 is bidirectional, consisting of a reductase activity and a dehydrogenase activity (6). The rate is most easily measured as B ([³H]-corticosterone) to A ([³H]-11-dehydrocorticosterone) conversion. As 11 β -reductase activity predominates in intact cells and tissues (6, 9), enzyme activity was assessed by the rate of B to A conversion (6, 9, 13). *, $P < 0.05$ compared with non-Tg mice in each fat tissue. (B) Adipose tissue corticosterone (CORT) concentration [14-week-old male non-Tg ($n = 9$) and Tg ($n = 8$) mice] was determined by methanol extraction followed by radioimmunoassay (Rat CORT RIA kit, ICN Pharmaceuticals) (15, 16). Mes, mesenteric fat; Epi, epididymal fat. Values were expressed as mean \pm SEM; *, $P < 0.01$ compared with non-Tg mice. (C) Body weight curves for male mice on low- or high-fat diet. When mice were 6 weeks of age, non-Tg and Tg mice were divided into two separately housed groups. One group was given a high-fat diet containing 45% fat (D12451, Research Diets, New Brunswick, NJ), and the second group was given a low-fat diet (D12450, Research Diets) containing 10% fat. Body weight and food intake were measured weekly. \blacklozenge , non-Tg mice fed a low-fat diet; \blacktriangle , Tg mice fed a low-fat diet; \blacksquare , non-Tg mice fed a high-fat diet; \bullet , Tg mice fed a high-fat diet ($n = 7$ in each group). Values were expressed as mean \pm SEM. * (Tg



mice fed a high-fat diet, $P < 0.001$ compared with non-Tg mice fed a high-fat diet; \dagger (Tg mice fed a low-fat diet), $P < 0.001$ compared with non-Tg mice fed a low-fat diet. (D) Gross appearance of 18-week-old male non-Tg and Tg mice. Ventral and dorsal views show loss of constriction of waist and larger abdomen in Tg mice. (E) Comparison of fat depot weight between non-Tg and Tg mice. Weight of unilateral epididymal, subcutaneous abdominal, and mesenteric fat depots in 16-week-old male non-Tg and Tg mice ($n = 6$ in each group) was measured as in (34). The ratio (Tg compared with non-Tg) in each fat depot were expressed as mean \pm SEM. (F) Fat weight in whole body (Wh.) and abdominal region (Abd.) assessed by DEXA (18) (Lunar Corporation, Madison, WI) (left). LF, low-fat diet; HF, high-fat diet. Values were expressed as mean \pm SEM; *, $P < 0.01$ compared with non-Tg mice; \dagger , $P < 0.005$ compared with non-Tg mice in respective diet (18-week-old male mice, $n = 8$ in each group). Fat weight in Abd./Wh.(%) (right). *, $P < 0.005$ compared with non-Tg mice; \dagger , $P < 0.01$ compared with non-Tg mice in respective diet.

REPORTS

All mice studied were inbred FVB strains crosses, wild type or hemizygous for the transgene. Ribonuclease (RNase) protection assays with a rat-based cRNA probe can differentiate the transgene-derived (rat) mRNA from endogenous murine 11 β HSD-1 mRNA. The transgene-derived transcript was expressed equivalently in adipose tissue from subcutaneous abdominal, epididymal, mesenteric, and interscapular brown adipose tissue (BAT) depots but was absent in brain, liver, skeletal muscle, and kidney of transgenic (Tg) mice. In line 7 male mice, in which all studies were performed unless otherwise noted, transgene-derived mRNA was increased sevenfold compared with endogenous mRNA (Web fig. 2). 11 β HSD-1 activity (6, 9, 13) was 2.4-fold increased in subcutaneous abdominal fat ($P < 0.03$) and 2.7-fold increased in epididymal fat ($P < 0.01$), respectively (Fig. 1A). In adipose tissue, the fold increase in aP2/11 β HSD-1 Tg mice was comparable

to that seen in leptin-deficient obese *ob/ob* mice and in obese humans (7), demonstrating that the extent of transgenic amplification of 11 β HSD-1 activity in aP2/11 β HSD-1 mice is physiologically relevant.

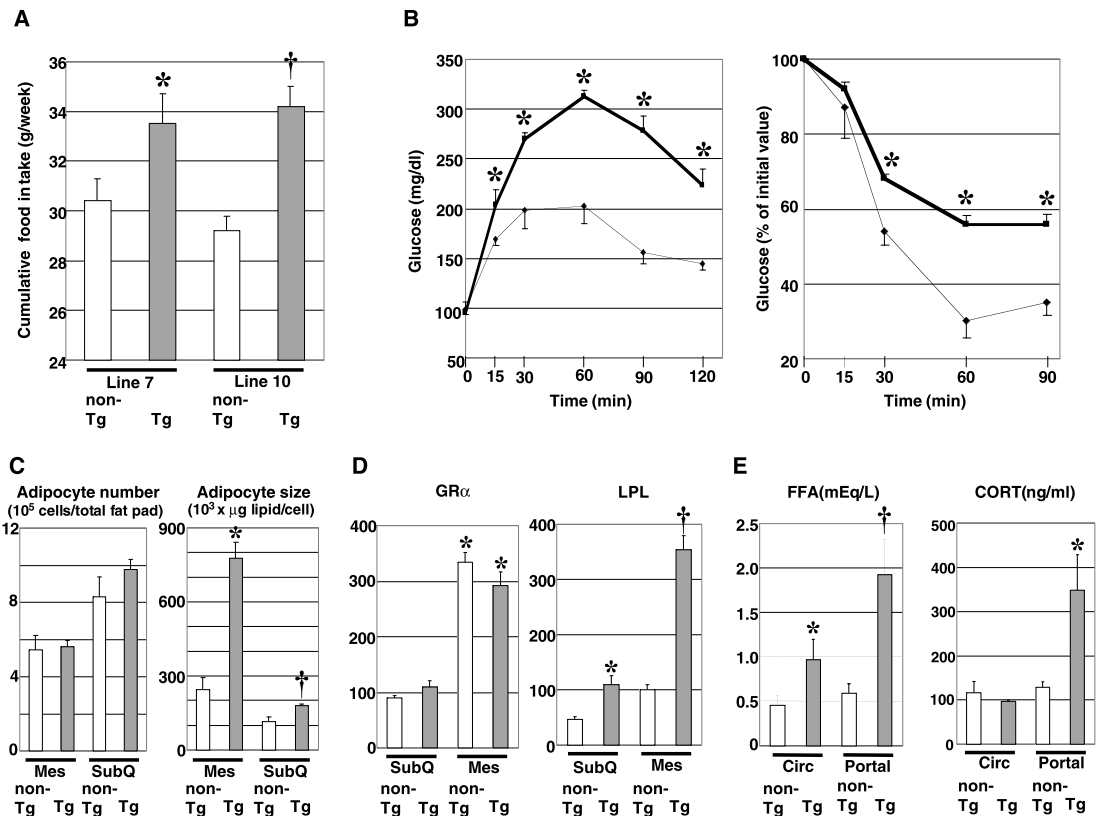
To address glucocorticoid metabolism in Tg mice, we measured corticosterone concentrations in adipose tissue and in serum. In two lines (7 and 10), serum corticosterone levels, measured under nonstressed conditions (14), were similar to those in control mice [117 ± 25 and 119 ± 4 ng/ml in non-Tg mice ($n = 8$) compared with 96 ± 13 and 104 ± 13 ng/ml in Tg mice ($n = 10$), respectively]. All values in the present study were expressed as mean \pm SEM]. In contrast, corticosterone concentrations in adipose tissue (15, 16) were significantly elevated (~ 15 to 30% increase compared with non-Tg mice, $P < 0.01$), reflecting increased local conversion of corticosterone (Fig. 1B). To confirm that corticosterone levels in the peripheral

circulation were not increased, we assessed several parameters that reflect the consequences of circulating glucocorticoids including thymic weight, bone mineral density, lean body mass weight, and linear growth; none were altered in Tg mice (Web note 1) (17).

From weaning to 9 weeks of age, body weights of non-Tg and Tg male mice fed normal (low-fat) diets were indistinguishable. However, weights diverged after 9 weeks and by 15 weeks of age, Tg mice weighed 16% more than non-Tg mice (Fig. 1C). The Tg showed increased sensitivity to weight gain on a high-fat diet. At 15 weeks of age, the body weight of Tg mice fed a high-fat diet for 9 weeks was 40.2 ± 1.2 g, which exceeded that of Tg mice fed a low-fat diet (32.5 ± 0.9 g, $P < 0.001$), non-Tg mice fed a high-fat diet (33.3 ± 0.7 g, $P < 0.001$), and non-Tg mice fed a low-fat diet (28.8 ± 0.5 g, $P < 0.0005$). The $24 \pm 1.7\%$ weight gain in Tg mice fed a high-fat diet was greater than the

Fig. 2. Metabolic phenotype in aP2/11 β HSD-1 transgenic mice.

(A) Cumulative food intake (g/week) in line 7 and line 10 mice (male, 14 weeks of age, $n = 9$ in each group). Values were expressed as mean \pm SEM. *, $P < 0.05$ compared with non-Tg mice (line 7); †, $P < 0.01$ compared with non-Tg mice (line 10). (B) Profile of intraperitoneal glucose tolerance test (1 mg of glucose per kg of body weight in awake mice after a 12-hour fast) [line 7, 18-week-old male Tg mice ($n = 8$) (■) and non-Tg ($n = 10$) (◆)] (left) and insulin tolerance test (0.75 U insulin per kg of body weight after a 6-hour fast) (right) (35). Values were expressed as mean \pm SEM; *, $P < 0.005$ compared with non-Tg mice. Data were assessed by analysis of variance (ANOVA) with repeated measures analysis (Statview 4.01; Abacus Concepts). (C) Adipocyte number and size in mesenteric and subcutaneous adipose tissue from 16-week-old male non-Tg and Tg mice ($n = 3$ in each group) were assessed as in (35). Values were expressed as mean \pm SEM; *, $P < 0.01$ compared with non-Tg mice; †, $P < 0.05$ compared with non-Tg mice. (D) Glucocorticoid receptor α isoform (GR α) (20) and LPL (27) mRNA expression in adipose tissue from 18-week-old non-Tg and Tg mice ($n = 5$ in each group). Specific mRNA for GR α was determined by quantitative reverse transcription (RT)-³²P polymerase chain reaction (PCR) with sense (5'-TGCTATGCTTTGCTCCTGATCTG-3') and antisense (5'-TGT-CAGTTGATAAACCGCTGCC-3') primers. LPL mRNA was determined by Northern blot. The β -actin mRNA were determined by RNase protection assay (HybSpeed RPA kit; Ambion, Austin,



TX). The results were normalized to the signal generated from β -actin mRNA. Values were expressed as mean \pm SEM. GR α : *, $P < 0.001$ compared with non-Tg SubQ or Tg SubQ, respectively. LPL: *, $P < 0.01$ compared with non-Tg SubQ; †, $P < 0.001$ compared with non-Tg Mes. (E) Portal FFA (left) and corticosterone (right) levels in non-Tg and Tg mice (20-week-old male mice, $n = 8$ in each group). Venous blood was taken (~ 200 μ l/mouse) from the proximal end of the portal vein with a 28G small syringe. Values were expressed as mean \pm SEM. FFA: *, $P < 0.005$ compared with non-Tg systemic circulation (Circ); †, $P < 0.001$ compared with non-Tg portal vein (Portal). Corticosterone: *, $P < 0.01$ compared with non-Tg Portal.

REPORTS

16 ± 0.6 % weight gain in non-Tg mice fed a high-fat diet ($P < 0.001$). Female Tg mice were not evaluated in the present study. External examination of the Tg mice suggested a prominent abdominal component to the weight gain (Fig. 1D). To evaluate the distribution of adiposity in Tg mice, we measured the weight of three different fat depots (Fig. 1E). Visceral fat is defined as fat depots located in the area of the portal circulation and is chiefly made up of omental and mesenteric fat (5). As mesenteric fat has a considerable amount of tissue and is easily isolated, the weight of mesenteric fat was measured as a representative of visceral fat (3, 5). The weight of unilateral epididymal adipose tissue did not differ between non-Tg and Tg mice [255 ± 14 mg (non-Tg) compared with 275 ± 12 (Tg)], and there was a small but significant increase in subcutaneous abdominal adipose tissue [1112 ± 75 mg (non-Tg) compared with 1432 ± 102 (Tg), $P < 0.05$]. In contrast, the weight of mesenteric adipose tissue was strikingly increased in Tg mice (795 ± 26 mg) compared with non-Tg mice (215 ± 14) ($P < 0.001$). Similar findings were observed in an additional independent line "10" [Web notes 2 and 3].

We also used dual energy x-ray absorptiometry (DEXA) (18) to measure the amount of fat in the whole body or in the abdominal region, defined as the area between the lower border of the thoracic rib cage and the upper border of the pelvic cavity (Fig. 1F). This region contains several fat depots, including visceral, retroperitoneal, and surrounding subcutaneous fat (3, 5, 18). In non-Tg mice at 18 weeks of age on low-fat diets, whole body and abdominal adipose tissue weight were 4.85 ± 0.22 g and 1.35 ± 0.16 g, respectively, whereas these weights in Tg mice were

7.97 ± 0.6 g and 3.0 ± 0.14 g, respectively. Accordingly, 27.5 ± 2.1% of adipose weight was in the abdominal region in non-Tg mice, compared with 37.9 ± 1.2% in Tg mice ($P < 0.005$). Fat accumulation in the abdominal region of non-Tg mice on high-fat diets was comparable to that in Tg mice on low-fat diets, and the ratio was further exaggerated in Tg mice fed high-fat diets. Thus, modest overexpression of 11 β HSD-1 in all adipose tissue produces disproportionate accumulation of visceral fat depots.

To examine the basis for increased energy balance in these mice, we monitored food consumption (Fig. 2A). Food intake was increased by 10.2 ± 0.7% ($P < 0.05$) and 17.1 ± 1.2% ($P < 0.01$), respectively, in lines 7 and 10, and this paralleled the increase in body weight (line 7, 10.2 ± 1.3% and line 10, 21.0 ± 2.5%). Thus, in addition to altering body fat distribution, adipose overexpression of 11 β HSD-1 engenders systemic alterations that result in hyperphagia.

Despite relatively modest degrees of overall obesity in Tg mice fed low-fat diets, the mice were markedly hyperglycemic [blood glucose fed ad libitum: 111 ± 6 mg/dl (non-Tg) compared with 164 ± 5 (Tg), $P < 0.001$] and hyperinsulinemic [230 ± 17 pg/ml (non-Tg) compared with 974 ± 254 (Tg), $P < 0.03$]. Intraperitoneal glucose and insulin tolerance testing in line 7 revealed pronounced glucose intolerance and insulin resistance (Fig. 2B). Similar findings were observed in a second independent line (Web note 4). Serum levels of free fatty acids (FFA), triglyceride, and leptin were also significantly increased (Table 1, top). Consistent with the notion that glucocorticoids are potent secretagogues of leptin from adipose tissue (19), leptin levels in Tg mice were disproportionately elevated

as assessed by the ratio of leptin (pg/ml)/body fat (g): 412 ± 96 (non-Tg) compared with 856 ± 130 (Tg), $P < 0.01$, suggesting that leptin resistance developed in Tg mice.

Although there was no difference between non-Tg and Tg mice in adipocyte number in mesenteric or subcutaneous abdominal fat depots, adipocyte size in these depots was increased 3.2-fold ($P < 0.006$) and 1.5-fold ($P < 0.05$) in Tg mice compared with non-Tg mice (Fig. 2C). Consistent with previous reports (3–5), the levels of glucocorticoid receptor α isoform (GR α) (20) mRNA were threefold higher in mesenteric compared with subcutaneous adipose tissue of both non-Tg and Tg mice ($P < 0.001$) (Fig. 2D). Enhanced GR α expression in visceral fat may account, at least in part, for the exaggerated accumulation of fat in this depot, despite similar overexpression of 11 β HSD-1 in all fat depots. Lipoprotein lipase (LPL) mRNA, which is known to be upregulated by glucocorticoids (21), was significantly increased in mesenteric adipose tissue of Tg mice (3.5-fold, $P < 0.001$) and less so in subcutaneous adipose tissue (2.4-fold, $P < 0.01$) (Fig. 2D). LPL overexpression can drive lipid accumulation in adipose depots (3, 5, 22).

We also studied the expression of adipose genes that are known or suspected to influence systemic metabolic pathways (Table 1, bottom). Adipocyte complement-related protein of 30 kD, (Acrp30)-AdipoQ (23), has been suggested to serve as an insulin-sensitizing factor (24). The mRNA level in mesenteric fat from Tg mice was markedly decreased, consistent with a role for this factor in the insulin-resistant state. The mRNA for resistin, which has been suggested to be involved in glucose homeostasis (25), was significantly decreased in Tg mice. Angiotensinogen mRNA, which is up-regulated by glucocorticoids (26), was substantially increased in Tg mice. Mitochondrial uncoupling protein-1 (UCP-1) mRNA (27) in interscapular BAT, which is down-regulated by glucocorticoids (28), was significantly decreased in Tg mice, suggesting a possible role for decreased BAT function in energy dysregulation in this model. Tumor necrosis factor- α (TNF- α), a fat cell-derived cytokine that can cause insulin resistance (3, 22), was significantly elevated in serum of Tg mice compared with non-Tg mice [39 ± 1.1 pg/ml (non-Tg) compared with 76 ± 11.2 pg/ml (Tg), $P < 0.02$].

In patients with the metabolic syndrome, considerable evidence suggests that increased FFA draining from visceral adipose tissue into the portal circulation contributes to hepatic insulin resistance (3, 5, 29). Portal FFA levels were increased by 3.3-fold in Tg mice ($P < 0.001$) (Fig. 2E). Because visceral fat produces active corticosterone through 11 β HSD-1, we considered the possibility that

Table 1. Metabolic parameters and adipocyte gene expression in 18-week-old male mice. Serum free fatty acids (FFA) and triglyceride were measured by NEFA-C kit and Triglyceride-E kit (Wako Chemicals, Richmond, VA). Leptin was determined by radio immunoassay (Linco Research, St. Louis, MO). Values were expressed as mean ± SEM. The mRNA for Acrp30-AdipoQ (23) and β -actin were determined by RNase protection assays (HybSpeed RPA kit, Ambion, Austin, TX). Resistin (25) and angiotensinogen (26) mRNA were determined by quantitative RT-³²P PCR with the following primers. Resistin: sense, 5'-ATGAAGAACCCTTCATTTCC-3'; antisense, 5'-CTTGACACTGGCAGTGACA-3'; angiotensinogen: sense, 5'-CCTGAAGGCCACCATCTCT-3'; antisense, 5'-GATCATTGGCAGCTGGGAG-3'. Mitochondrial uncoupling protein-1 (UCP-1) mRNA was determined by Northern blot (27). The results were normalized to the signal generated from β -actin mRNA and expressed as mean ± SEM. Values in Tg mice were expressed as a percentage of those in non-Tg mice. mesenteric, mesenteric adipose tissue, BAT, brown adipose tissue.

Metabolic parameters	non-Tg (n = 9)	Tg (n = 9)	P value
Serum free fatty acids (mEq/liter)	0.31 ± 0.03	0.76 ± 0.06	$P < 0.0001$
Serum triglyceride (mg/dl)	112 ± 10	181 ± 14	$P < 0.02$
Serum leptin (pg/ml)	1996 ± 473	5231 ± 797	$P < 0.02$
Adipose gene expression	non-Tg (n = 5)	Tg (n = 5)	P value
Acrp30-AdipoQ (mesenteric)	100 ± 19	42 ± 1.4	$P < 0.04$
Resistin (mesenteric)	100 ± 7	70 ± 5.1	$P < 0.03$
Angiotensinogen (mesenteric)	100 ± 2	372 ± 21	$P < 0.001$
UCP-1 (interscapular BAT)	100 ± 12	63 ± 10	$P < 0.05$

REPORTS

visceral adipocytes of transgenic mice release sufficient corticosterone into the portal vein to alter the levels exposed to the liver. Indeed, portal vein corticosterone levels in Tg mice were increased 2.7-fold [129 ± 11.1 ng/ml (non-Tg) compared with 349 ± 79.5 ng/ml (Tg), $P < 0.01$] (Fig. 2E). Thus, visceral fat may affect hepatic metabolism by portal production of glucocorticoids as well as FFA.

Glucocorticoids regulate adipose tissue differentiation, function, and distribution, and their systemic excess produces a syndrome of central obesity with diabetes, hyperlipidemia, and hypertension, known as Cushing's syndrome (3–5). Although subtle alterations in the endocrine hypothalamic pituitary adrenal (HPA) axis have been reported in some studies of obesity (4, 5, 30), these have been controversial, and no clear role for increased circulating glucocorticoids in visceral obesity has emerged. On the other hand, a role for increased local cortisol reactivation in human obesity is suggested by several findings (5–7, 31). 11β HSD-1 activity is higher in human visceral compared with subcutaneous adipose tissue (31), and reactivation of cortisone to cortisol is increased selectively in adipose tissue of obese humans, while impaired in liver (7). Similar findings were reported in obese Zucker rats (8). The thiazolidinedione (TZD) class of antidiabetic agents that are ligands for peroxisome proliferator-activated receptor (PPAR) γ markedly reduce adipocyte 11β HSD-1 mRNA and activity both in vivo and in vitro (32). Because TZDs preferentially reduce visceral fat accumulation in humans (3, 5, 22, 33), suppression of adipose 11β HSD-1 by TZDs could be a mechanism for this fat redistribution and may play a role in their antidiabetic effects.

Our finding that a modest increase in the activity of 11β HSD-1 in adipose tissue of mice is sufficient to cause hyperphagia with visceral obesity and its most critical metabolic complications demonstrates that glucocorticoid-dependent adipocyte pathways have an unexpectedly major impact on systemic biology. Adipose tissue of obese humans is reported to have increased activity of 11β HSD-1 of similar or greater magnitude than that observed in our transgenic mice (7). These findings strongly suggest that increased adipocyte 11β HSD-1 is a common molecular mechanism for visceral obesity and the metabolic syndrome and may be an exciting pharmaceutical target for the treatment of this prevalent disorder.

References and Notes

- P. G. Kopelman, *Nature* **404**, 635 (2000).
- J. Vague, *Am. J. Clin. Nutr.* **4**, 20 (1956).
- C. T. Montague, S. O'Rahilly, *Diabetes* **49**, 883 (2000).
- P. Bjorntorp, R. Rosmond, *Nutrition* **16**, 924 (2000).
- B. L. Wajchenberg, *Endocr. Rev.* **21**, 697 (2000).
- J. R. Seckl, B. R. Walker, *Endocrinology* **142**, 1371 (2001).
- E. Rask et al., *J. Clin. Endocrinol. Metab.* **86**, 1418 (2001).
- D. E. W. Livingstone et al., *Endocrinology* **141**, 560 (2000).
- Y. Kotelevtsev et al., *Proc. Natl. Acad. Sci. U.S.A.* **94**, 14924 (1997).
- A. K. Agarwal et al., *J. Biol. Chem.* **264**, 18939 (1989).
- S. R. Ross, R. A. Graves, B. M. Spiegelman, *Genes Dev.* **7**, 1318 (1993).
- Supplementary data are available on Science Online at www.sciencemag.org/cgi/content/full/294/5549/2166/DC1.
- A. Napolitano et al., *J. Steroid Biochem. Mol. Biol.* **64**, 251 (1998).
- R. S. Ahima et al., *Nature* **382**, 250 (1996).
- J. Szymczak et al., *Steroids* **63**, 319 (1998).
- M. H. Rahimy, N. Bodor, J. W. Simpkins, *J. Steroid Biochem.* **33**, 179 (1989).
- R. Rooman et al., *J. Endocrinol.* **163**, 543 (1999).
- T. R. Nagy, A. L. Clair, *Obes. Res.* **8**, 392 (2000).
- R. S. Ahima, J. S. Flier, *Annu. Rev. Physiol.* **62**, 413 (2000).
- B. D. Abbot et al., *Toxicol. Sci.* **47**, 76 (1999).
- J. Kobayashi et al., *Br. J. Clin. Pharmacol.* **47**, 433 (1999).
- G. Fruhbeck et al., *Am. J. Physiol. Endocrinol. Metab.* **280**, E827 (2001).
- P. E. Scherer et al., *J. Biol. Chem.* **270**, 26746 (1995).
- T. Yamauchi et al., *Nature Med.* **7**, 941 (2001).
- C. M. Steppan et al., *Nature* **409**, 307 (2001).
- J. Aubert et al., *Biochem. J.* **328**, 701 (1997).
- N. Satoh et al., *Neurosci. Lett.* **249**, 107 (1998).
- A. M. Strack, M. J. Bradbury, M. F. Dallman, *Am. J. Physiol.* **268**, R183 (1995).
- A. H. Kissebah, A. N. Peris, *Diabetes Metab. Rev.* **5**, 83 (1989).
- R. Rosmond, M. F. Dallman, P. Bjorntorp, *J. Clin. Endocrinol. Metab.* **83**, 1806 (1998).
- I. J. Bujalska, S. Kumar, P. M. Stewart, *Lancet* **349**, 1210 (1997).
- J. Berger et al., *J. Biol. Chem.* **276**, 12629 (2001).
- T. Kawai et al., *Metabolism* **48**, 1102 (1999).
- N. Tsuboyama-Kasaoka et al., *Diabetes* **49**, 1534 (2000).
- E. D. Abel et al., *Nature* **409**, 729 (2001).
- Supported by grants from NIH (J.S.F.) and Eli Lilly (J.S.F.), a programme grant from the Wellcome Trust (J.R.S. and J.J.M.), and grants from the Transgenic Core Facility of the Boston Obesity Nutrition Research Center and Animal Physiology Core of the Diabetes Endocrinology Research Center. H.M. held research fellowships from Uehara Memorial Foundation, Wellfide Research Foundation, and Yamanouchi Foundation for Research on Metabolic Disorders. We thank K. Araki, B. B. Kahn, J. K. Hamm, Y.-B. Kim, Y. Minokoshi, I. Shimomura, R. S. Ahima, N. Tsuboyama-Kasaoka, H. Fang, and B. R. Walker for their invaluable advice and L. Ungsunann, L. Ramage, J. Lawitts, M. Meikle, O. Peroni, E. Hadro, and R. Rossi for their excellent assistance.

17 September 2001; accepted 25 October 2001

Rapid Killing of *Streptococcus pneumoniae* with a Bacteriophage Cell Wall Hydrolase

Jutta M. Loeffler, Daniel Nelson, Vincent A. Fischetti*

Nasopharyngeal carriage is the major reservoir for *Streptococcus pneumoniae* in the community. Although eliminating this reservoir would greatly reduce disease occurrence, no suitable intervention has been available for this purpose. We show here that seconds after contact, a purified pneumococcal bacteriophage lytic enzyme (Pal) is able to kill 15 common serotypes of pneumococci, including highly penicillin-resistant strains. In vivo, previously colonized mice revealed undetectable pneumococcal titers 5 hours after a single enzyme treatment. Pal enzyme had little or no effect on microorganisms normally found in the human oropharynx, and Pal-resistant pneumococci could not be detected after extensive exposure to the enzyme.

Streptococcus pneumoniae remains one of the most challenging human pathogens because of the morbidity and mortality it causes in young children, the elderly, and in immunocompromised patients. The asymptomatic carrier state, particularly in children, is thought to be the major reservoir of the pathogen. Pneumococci account for several million cases of acute otitis media and an estimated 60,000 cases of invasive disease in the United States each year, with a mortality of 10% (1). Because of the worldwide increase of resistance to multiple antibiotics in pneumococci, treatment has become more difficult than in the past.

Laboratory of Bacterial Pathogenesis, The Rockefeller University, New York, NY 10021, USA.

*To whom correspondence should be addressed. E-mail: vaf@mail.rockefeller.edu

Prevention of pneumococcal disease relies today on vaccination of the susceptible population. However, vaccination encounters a number of problems such as the limited quantity of serotypes in the pediatric formulation, incomplete protection against colonization, and selection of nonvaccine serotypes (2, 3). There is need for an alternative preventive strategy for situations where vaccination is insufficient, impossible, or inefficient. Eradication or even reduction of nasopharyngeal carriage is likely to have a major impact on the transmission of *S. pneumoniae* and the incidence of infection. Antibiotic prophylaxis in controlled surroundings has shown limited success but carries the risk of selective pressure resulting in an increase of resistant strains (4). Until now, there has been no substance that can specifically reduce the number of pneumococci carried on human mu-